HHS Public Access

Author manuscript

Chem Phys Lett. Author manuscript; available in PMC 2016 October 01.

Published in final edited form as:

Chem Phys Lett. 2015 October 1; 638: 56–60. doi:10.1016/j.cplett.2015.08.026.

Probing environmentally significant surface radicals: Crystallographic and temperature dependent adsorption of phenol on ZnO

Chad A. Thibodeaux[a], **E.D. Poliakoff**[a], **Orhan Kizilkaya**[b], **Matthew C. Patterson**[c], **Mark F. DiTusa**[c], **Richard L. Kurtz**[b,c], and **P.T. Sprunger**[c]

Chad A. Thibodeaux: icepilot28@gmail.com; E.D. Poliakoff: epoliak@lsu.edu; Orhan Kizilkaya: orhan@lsu.edu; Matthew C. Patterson: mpatt15@tigers.lsu.edu; Mark F. DiTusa: mditus1@gmail.com; Richard L. Kurtz: rlkurtz@lsu.edu; P.T. Sprunger: Sprunger-phils@lsu.edu

[a]Louisiana State University, Department of Chemistry, 232 Choppin Hall, Highland Road, Baton Rouge, LA 70803, United States

[b]Louisiana State University, Center for Advanced Microstructures and Devices, 6980 Jefferson Hwy., Baton Rouge, LA 70806, United States

[c]Louisiana State University, Department of Physics and Astronomy, 202 Nicholson Hall, Tower Dr., Baton Rouge, LA 70803, United States

Abstract

Environmentally persistent free radicals (EPFRs) are toxic organic/metal oxide composite particles that have been discovered to form from substituted benzenes chemisorbed to metal oxides. Here, we perform photoelectron spectroscopy, electron energy loss spectroscopy, and low energy electron diffraction of phenol chemisorbed to ZnO(1 0 $\underline{1}$ 0) and (0 0 0 $\underline{1}$)-Zn to observe electronic structure changes and charge transfer as a function adsorption temperature. We show direct evidence of charge transfer from the ZnO surfaces to the phenol. This evidence can help gain a better understanding of EPFRs and be used to develop possible future remediation strategies.

1. Introduction

The adsorption of aromatic molecules on metal oxide surfaces continues to attract attention due to their potentially significant environmental impacts [1–4]. In particular, recent experiments have demonstrated that when certain classes of substituted benzenes chemisorb to metal oxide surfaces, such as ZnO, environmentally persistent free radicals (EPFRs) are formed. EPFRs are thermally activated radicals with half-lives of hours to days under ambient conditions and indefinitely under vacuum [5–9]. The term EPFR refers to these composite organic/metal oxide pollutant particles. Specifically, ZnO is known to form the longest-lived EPFRs with half-lives up to 73 days based on EPR results where *g*-values are consistent with aromatic type radicals [7]. Moreover, these previous EPR results indicate that EPFR formation is thermally activated (>150 °C). Previous *ab initio* calculations

Correspondence to: P.T. Sprunger, Sprunger-phils@lsu.edu.

associate this exceptional stability and low reactivity to a chemisorption/charge-transfer mechanism which results in resonance stabilization including both oxygen and carbon-centered radicals [10]. The association of EPFRs with toxic airborne particulate matter is important because they pose serious health consequences to humans [11–20]. Developing a detailed model of the thermally activated mechanism of EPFR formation on metal oxides is a necessary first step in understanding their toxicity and in guiding strategies for remediation. To gain key insights into real world systems we employ a model system to probe a key step in EPFR formation, namely, the temperature-dependent chemisorption of phenol on well-defined ZnO surfaces. Because single crystal ZnO has few low-energy crystallographic faces [21,22], this is an ideal model system to obtain comprehensive information that closely represents nanoparticle powder samples, which have been used in previous studies [4–8]. This study aims to understand the detailed atomic and electronic structure of EPFRs formed on two differing ZnO crystallographic faces namely the (1 0 $\underline{1}$ 0) and (0 0 0 $\underline{1}$)-Zn surfaces as a function of temperature. Our experimental data strongly suggests that upon adsorption of phenol, a known EPFR precursor, there is a charge transfer away from both ZnO surfaces toward the phenol, which is inconsistent with a previously proposed mechanism of EPFR formation [23]. Moreover, surface spectroscopic data, which probe the electronic properties of the adsorbed phenol, reveal that there is a significant difference between adsorption at room temperature versus elevated temperatures for the (0 0 0 $\underline{1}$) surface only. Additionally, employing surface diffraction, we show that the adsorption of phenol (1 0 $\underline{1}$ 0) surface results in a semi-ordered atomic superstructure.

To date, only generic mechanisms which lack atomistic details have been proposed for EPFR formation on metal oxide surfaces [5,6,24]. The mechanisms consist of an initial chemisorption of the EPFR precursor molecule, typically alcohol or halogenated aromatic systems, to the surface followed by elimination of water or HCl and consequent charge transfer between the molecule and metal oxide surface. During this latter activated process, a concurrent reduction of the metal and EPFR formation occurs. In this context, interactions between phenol and ZnO become interesting because of the limited stable oxidation states of Zn (a +1 state is non-existent). This motivates the importance to understand the atomic and electronic structure in detail. Furthermore, our electronic and structural studies can be used by theorists as a guidepost to aid in developing a clearer picture of the interactions between aromatic organics and transition metal oxides taking into account both morphology/symmetry and electronic details.

In this study, we perform low energy electron diffraction (LEED), electron energy loss spectroscopy (EELS), and ultraviolet photoelectron spectroscopy (UPS), of phenol adsorbed at low temperature (90 K), room temperature, and at 220 °C on non-polar ZnO(1 0 $\underline{1}$ 0) and polar ZnO(0 0 0 $\underline{1}$)-Zn single crystal surfaces as surrogate model systems for EPFR formation. Using UPS we were able to observe band bending toward the Fermi level indicating charge transfer from the ZnO surfaces to the phenol at both room temperature and 220 °C, which differs from previously proposed EPFR formation mechanisms. Moreover, EELS measurements are used to probe low-energy electronic transitions of chemisorbed phenol as a function of temperature to compliment the UPS measurements. The UPS and EELS measurements together reveal that the ring of phenol chemisorbed on (1 0 $\underline{1}$ 0) likely remains intact and the phenol chemisorbed to the (0 0 0 $\underline{1}$)-Zn shows significant changes that

indicate that EPFR formation may favor the Zn-terminated surfaces. The LEED measurements also show significant differences between the adsorbate atomic structure arrangement two surfaces. On the (1 0 $\underline{1}$ 0) surface chemisorbed phenol forms a semi-ordered superstructure while phenol on the (0 0 0 $\underline{1}$)-Zn surface is completely disordered.

This investigation is part of a larger program to study EPFR precursors on transition metal oxides. It is clear from the results that will be presented that the simple unverified mechanism does not describe all systems where EPFRs are known to form, although recent experimental studies have demonstrated charge transfer from the adsorbed organic species to the metal oxide in the direction proposed by the generic mechanism [23]. Experimental and theoretical studies are required to generate insights into other EPFR/metal oxide systems and this study can help those who are interested in such systems. By performing detailed studies of the atomic and electronic structure of such systems a clearer picture maybe obtained to understand how each system behaves individually, highlighting their similarities and their differences.

2. Materials and methods

All experiments were performed in ultra-high vacuum (UHV) systems with base pressures below 2×10^{-10} Torr. ZnO(1 0 $\underline{1}$ 0) and ZnO(0 0 0 $\underline{1}$)-Zn samples (10 mm × 10 mm × 1 mm) were purchased from MTI Corporation and cleaned in UHV by several cycles of 1.5 keV Ne ion bombardment at 5×10^{-5} Torr for 45 min followed by 30 min annealing at 650 °C. EELS spectra were taken before dosing with phenol to ensure cleanness of the sample wherein only phonons and bulk band gap (~3.7 eV) features were identified. Adsorption of the EPFR precursor was accomplished by introducing phenol vapor into the vacuum chamber using a standard leak valve. The phenol was purified by several freeze-pump-thaw cycles. For dosing at elevated temperatures, the respective crystal was brought to a given temperature in vacuum as measured with a type K thermocouple. Upon cooling to room temperature, data was acquired. The EELS measurements, using a LK2000 EELS spectrometer employed a primary beam energy of 30 eV with a resolution of ~15 meV (measured by the FWHM of the elastically scattered electron beam in the specular direction) in specular geometry. When dosing at low temperature, the samples were exposed and spectra were collected while the sample was held at ~90 K. All EELS spectra were normalized to the height of the elastic peak.

All UPS measurements were performed using the 5 m toroidal grating monochromator (5m-TGM) beamline and UPS endstation at the Center for Advanced Microstructures and Devices (CAMD) at Louisiana State University, which are described in detail elsewhere [25]. A 50 mm hemispherical analyzer was used to acquire the normal emission spectra with 40 eV, 45° incident light. The Fermi edge was determined from the sputtered copper sample holder.

The electronic structure of molecular phenol was calculated using WIEN2k with a unit cell of 15 × 14 × 10 Å, ensuring enough vacuum space that the molecules are essentially isolated. Exchange-correlation potential used was the revised GGA of Perdew–Burke–Ernzerhof and the molecule was allowed to fully relax [26].

3. Results

Figure 1 shows the photoelectron spectra of phenol dosed at 220 °C on non-polar ZnO(1 0 1 0) (Figure 1a) and polar (0 0 0 1)-Zn (Figure 1c) terminated surfaces. On both clean ZnO surfaces we see a clear photoemission peak centered around 10.8 eV binding energy (BE) due to the Zn 3*d* emission. The remaining intensity between 4 and 8 eV BE is attributed to the O 2*p* and the Zn 4*s* electrons, respectively. The (1 0 1 0) surface has an additional peak at approximately 6 eV, which has been attributed to a hybridization of the Zn 4*s*-O 2*p* orbitals [27]. Upon deposition of 100 L of phenol at 220 °C, a shoulder appears on the upper edge of the O *2p* band at binding energy of approximately 2.5 eV on the (1 0 1 0) surface and 3.0 eV on the (0 0 0 1)-Zn surface. We assign this shoulder structure at the edge of the valence band maximum (3.7 BE) to be the phenol HOMO band, which primarily lies in the band gap of ZnO. This assignment is consistent with other aromatics on ZnO [28,29]. In addition, another peak emerges at approximately 14 eV that has been assigned to the phenol sigma orbitals [30]. The spectra for room temperature doses (not shown) were also obtained and the same spectral features appeared for both surfaces at the same binding energies as their higher temperature counterparts.

The inset of Figure 1 shows difference spectra between both clean and adsorbed surfaces. The difference spectra were obtained after a correction for band bending was performed (see discussion below) and after normalization to the hybrid peak for the (1 0 1 0) surface and the Zn 3*d* peak for the (0 0 0 1)-Zn surface. A comparison of the difference spectra between the two surfaces reveals a 0.5 eV shift to higher binding energy in the Zn terminated spectrum. The line shape of the phenol HOMO on the Zn terminated surface is also quite different. For the non-polar surface, two peaks are present that appear to be in good agreement with the calculated spectrum that are assigned to the HOMO at 2.5 eV and HOMO − 1 at 3.5 eV (see bottom spectrum of the inset). However, the Zn-terminated spectrum shows a clear difference with the calculation; Specifically, it appears that either one peak has disappeared or that the two peaks are merged together. Another significant difference between the clean and dosed photoelectron spectra is the 0.6 eV and 0.4 eV Zn 3*d* band bending for the (1 0 $\underline{1}$ 0) surface and the (0 0 0 $\underline{1}$)-Zn surface, respectively. This near surface, upward shift toward the Fermi edge (decreasing BE) is consistent with a charge transfer from the surface to the phenol [31,32].

Although UPS yields information of the near-surface valence structure, EELS provides a surface sensitive method to examine low energy electronic excitations. In combination with UPS, EELS measurements allow us to infer additional key details of the electronic structure of the phenol/ZnO system, Specifically the excitations of ZnO and phenol. Figure 2 shows EELS spectra of clean and dosed (1 0 $\underline{1}$ 0) and (0 0 0 $\underline{1}$)-Zn at the same conditions as Figure 1. The spectral range of 0.2–9.0 eV loss energy yields direct information on the ZnO low energy band gap, interband transition at 3.6 eV (as shown in Figure 2a and indicated by the dash-dot vertical line) and the low energy corresponding HOMO–LUMO transitions of phenol [33,34]. Also included is the spectrum from a non-polar surface with physisorbed phenol at −177 °C (b). At this low temperature multiple layers of phenol are condensed, effectively forming ‘phenol ice’. Figure 2b shows condensed phenol transitions at 3.7, 4.5, 5.7, and 6.5 eV, which are due to π–π* transitions and consistent with previous gas phase

measurements of phenol [34]. These excitations Specifically are between the HOMO/HOMO − 1 and LUMO/LUMO + 1/LUMO + 2 orbitals of phenol. The intense peak at 6.5 eV (indicated by a dotted vertical line in Figure 2) is similar to that of benzene, but is perturbed by the lone pair of electrons located on the oxygen causing a shift to lower energy [34].

Comparing spectra of 100 L adsorbed phenol on the (1 0 1 0) surface at room temperature and 220 °C (c and e), only small differences are observed. The room temperature spectrum (c) is shifted to lower loss energy from the 'phenol ice' (b) by 0.2 eV while the 220 °C (e) spectrum is shifted even further to lower energy by 0.4 eV. Other than these shifts in loss energy, overall the spectra for the (1 0 1 0) surface looks like slightly perturbed, but intact phenol. This corroborates well with the UPS data shown in Figure 1. There appears to be some temperature dependence on the adsorption of phenol on the non-polar surface. However, this only shifts the spectra to lower energy.

The (0 0 0 $\underline{1}$)-Zn surface, however, is significantly different from the (1 0 1 0) surface. Figure 2d, room temperature adsorption (100 L phenol) very closely resembles the non-polar surface (Figure 2c) under the same conditions. However, when the adsorption occurs at elevated temperature (220 °C) the spectrum (Figure 2f) shifts significantly to lower loss energy by 0.7 eV compared to Figure 2b. More importantly, EELS shows the intensity feature at 2.3 eV which is presumably due to additional transitions from the HOMO of phenol to the conduction band minimum (CB_{min}) of ZnO similar to the nitrocatechol system studied by Arnaud et al. [29]. Also, two very prominent peaks are observed at excitation energies of approximately 4.0 and 5.8 eV. These new peaks at 4.0 and 5.8 eV were also observed with nitrocatechol adsorbed to ZnO and were assigned to be the HOMO to LUMO and HOMO to LUMO + 1 transitions, respectively. Overall, EELS reveals that for the Zn-terminated surface, substantial changes occur between the phenol chemisorbed states at room temperature and 220 °C, while the non-polar surface shows slight changes between temperatures.

In addition to the electronic information yielded by UPS and EELS, information regarding the surface atomic structure is inferred from LEED. Figure 3 shows LEED patterns for the (1 0 $\underline{1}$ 0) and the (0 0 0 $\underline{1}$)-Zn surfaces before and after adsorption of 25 L of phenol at room temperature. The non-polar (1 0 $\underline{1}$ 0) surface is characterized by rows of zinc and oxygen dimers at top of the structural model in Figure 3e. As shown, equal numbers of zinc and oxygen atoms are present in the surface plane making it non-polar. This is in contrast to the polar (0 0 0 1) surfaces, indicated by the sides of the structural model in Figure 3e, which can be terminated with either all zinc (left) or oxygen atoms (right). A typical unreconstructed LEED pattern of ZnO(1 0 $\underline{1}$ 0) yields a (1 × 1) rectangular pattern (Figure 3a). The polar (0 0 0 $\underline{1}$)-Zn surface (Figure 3c) also yields a (1 × 1) pattern with six-fold symmetry, as previously reported in the literature [22,21]. When the (1 0 $\underline{1}$ 0) surface is exposed to 25 L of phenol at room temperature, as shown Figure 3b, a c(2 × 2) superstructure is observed with streaking along the (0 0 0 1) direction. This indicates that the phenol is ordered in the (1 $\underline{2}$ 1 0) direction but lacks long-range coherence, or order along the (0 0 0 1) direction. As seen in the structural ZnO model in Figure 3e, this (0 0 0 1) direction is perpendicular to the Zn O dimer rows. When the sample temperature is elevated

to 220 °C, the same streaking pattern appears (not shown). Upon additional exposure to phenol (beyond 25 L) the LEED pattern does not change indicating the surface is fully saturated at approximately 0.5 ML.

Unlike the non-polar surface that shows a streaking pattern upon exposure to 25 L phenol, LEED indicates that on the polar (0 0 0 $\underline{1}$)-Zn surface exhibits an overall increase in diffuse background occurs, as shown in Figure 3d. This suggests a clear distinction between the bonding on the two crystallographic surfaces. When the sample temperature is raised to 220 °C, the same diffuse background appears. For both surfaces there is a lack of temperature dependence with regard to LEED measurements.

4. Discussion

A significant observation in Figure 1 is the 0.6 eV and 0.4 eV band bending on the (1 0 $\underline{1}$ 0) surface and (0 0 0 $\underline{1}$)-Zn surface, respectively, upon adsorption of phenol. This type of behavior is not an uncommon phenomenon with ZnO, especially when molecules containing oxygen such as carbon monoxide, ethylene oxide, and methanol are adsorbed [32]. This type of band bending occurs when a molecule adsorbs to a weakly screened (non-metallic) surface. The molecular orbitals can either (1) accept charge from the surface, forming an electric field that pulls the bands ‘upward’ (toward the Fermi level) causing a shift to lower binding energy in photoelectron spectra, or (2) donate charge to the surface, forming an electric field that pulls the bands ‘downward’ (away from the Fermi level), shifting the photoelectron spectra to higher binding energy. Based on this idea, our PES results suggest direct evidence of a charge transfer from the ZnO to the phenol [31], which is somewhat unusual considering phenol is regarded as a poor electron acceptor. This observation has significant impact on the proposed mechanism of EPFR formation described earlier and that has been previously observed in other metal oxide systems [24]. This previously proposed mechanism indicates that charge is transferred from the adsorbate to metal oxide causing a partial reduction of the metal cation, however, the PES data of both phenol/ZnO systems indicate the reverse occurs. This could explain why EPFRs form on ZnO while no +1 oxidation state of Zn exists. This is confirmed by the lack of intensity of structure near the Fermi level indicating an absence of metallic Zn formation.

The UPS data adds additional insight into phenol bonding, namely the details of the HOMO structure near 2.5 eV. The inset in Figure 1 shows the difference spectra of both surfaces compared to a WIEN2k calculation of a single phenol molecule. The (1 0 $\underline{1}$ 0) surface closely matches the calculation suggesting that the phenyl ring of chemisorbed phenol remains intact on the (1 0 $\underline{1}$ 0) surface. However, details of the HOMO band(s) on the Zn-terminated surface are clearly different. It is not clear if a state is being depopulated or if degeneracy is being added to the phenol. Although EELS shows a temperature dependent structure both surfaces, there is a lack of temperature dependence on both surfaces with respect to the occupied states.

A comparison of the temperature dependent EELS spectra between the two surfaces shows significant differences. Comparing spectra in Figure 2b with 2c, 2d, and 2e, there is only a slight shift to lower loss energy by 0.2 and 0.4 eV. The dominant feature remains the π–π^*

transitions at 6.5, 6.3, and 6.1 eV [34]. Spectra seen in Figure 2c–e seem to reflect the presence of intact chemisorbed phenol on both surfaces since no spectral features change except for a slight shift in loss energy. Since the UPS shows no HOMO shifts with regard to temperature for each surface, yet the EELS does show shifts to lower loss energies as a function of temperature, this implies that the LUMOs decrease in energy as a function of temperature for both surfaces. Both UPS and EELS data support the observation that the phenyl ring of chemisorbed phenol is indeed intact on the (1 0 $\underline{1}$ 0) surface.

The high temperature adsorption of phenol on the polar surface (Figure 2f) is significantly different than any other spectrum in Figure 2. Not only does this spectrum have the largest π–π* transition shift of 0.7 eV compared to the 'phenol ice', but it also shows a low energy onset excitation at 2.3 eV. No other spectrum has this as an obvious feature and suggests the presence of a HOMO to metal oxide CB_{min} transition. This means that the phenol HOMO is inserted into the ZnO band gap. While it may be present in the (1 0 $\underline{1}$ 0) spectra, it is very low in intensity by comparison. The shift to lower energy also implies that the HOMO–LUMO gap has narrowed far more than on the other surface at the elevated temperature adsorption. This significant collapse could suggest that the polar Zn-terminated surface is more conducive for EPFR formation, which corroborates the UPS data in Figure 1.

Very few LEED patterns of aromatic organics on ZnO have been recorded [22]. Benzene on ZnO(1 0 $\underline{1}$ 0) was investigated using LEED by Poss et al. [35]. The authors found that benzene formed a well ordered c(2 × 2) superstructure with very sharp diffraction spots. Upon further adsorption, the LEED pattern changed to a c(4 × 3) structure indicating multilayer growth of benzene which is in contrast to phenol on the same (1 0 $\underline{1}$ 0) surface wherein no additional superstructures were observed at higher coverages. Moreover, the streaked c(2 × 2) superstructure remains upon dosing at higher temperatures (220 °C). As a comparison, benzene is believed to lay flat on the surface of ZnO(1 0 $\underline{1}$ 0) [22,35], however, it is suspected that phenol binds to the surface through the oxygen atom leaving the phenyl ring to orient itself in a random fashion leading to no long range coherence.

LEED indicates that phenol prefers to bond in a semi-ordered c(2 × 2) fashion on the (1 0 $\underline{1}$ 0) surface rather than on the (0 0 0 $\underline{1}$)- Zn. Since increasing the dosage of phenol beyond 25 L did not change the LEED pattern, this means that the (1 0 $\underline{1}$ 0) surface becomes fully saturated near 0.5 ML. This is of great importance for simulations since the bonding geometry can be quite different for both surfaces, which could have impacts on the electronic structure of the adsorbed phenol.

5. Conclusions

We have studied the electronic structure and adsorption ordering of the phenol/ZnO model system as a function of both crystallographic face dependence and temperature. We find that upon saturation doses of phenol at room temperature and 220 °C the resulting photoelectron spectra shift to lower binding energy due to band bending, suggesting a charge transfer away from the ZnO toward the chemisorbed phenol. This is contradictory to a previously proposed EPFR formation mechanism based on phenol chemisorbed to rutile TiO_2 (1 1 0) [24]. Our combined UPS with EELS experimental evidence shows evidence of the intact

phenyl ring of chemisorbed phenol on the ZnO(1 0 1 0) surface even at elevated temperatures. However, phenol chemisorbed to the polar Zn-terminated surface shows significant differences that could suggest EPFR formation is more favorable on that surface. UPS data also showed no temperature differences indicating similar occupied states structure for phenol at both RT and 220 °C. On the other hand, EELS consistently showed excitation shifts to lower loss energy. This means that the HOMO–LUMO gap decreases or collapses and hence only the LUMO states decrease in energy. LEED measurements also showed significant long-range structural differences between adsorption on the two surfaces. Whereas, phenol forms a semi-ordered c(2 × 2) superstructure on the (1 0 1 0) surface, it is disordered on the polar Zn-terminated surface. The LEED experiments also showed that phenol is fully saturated near 0.5 ML of phenol on the non-polar surface. This study should serve as a guidepost for future computational studies that wish to attempt to model radical formation on ZnO or other metal oxide systems.

Acknowledgements

The authors acknowledge support from the National Institute of Environmental Health Sciences Superfund Research Program through Grant No. P42 ES013648-03. Additionally, PTS and MFD acknowledge partial support from the National Science Foundation (NSF) EPSCoR Cooperative Agreement No. EPS-1003897 with additional support from the Louisiana Board of Regents. We also acknowledge the support of the staff of the CAMD synchrotron light source.

References

1. Sun M, Altarawneh B, Dlugogorski Z, Kennedy EM, Mackie JC. Environ. Sci. Technol. 2007; 41:5708. [PubMed: 17874777]
2. Evans CS, Dellinger B. Chemosphere. 2006; 63:1291. [PubMed: 16297959]
3. Milligan MS, Altwicker ER. Environ. Sci. Technol. 1996; 30:230.
4. Bandara J, Mielczarski JA, Kiwi J. Appl. Catal. B: Environ. 2001; 34:307.
5. Lomnicki S, Truong H, Vejerano E, Dellinger B. Environ. Sci. Technol. 2008; 42:4982. [PubMed: 18678037]
6. Vejerano E, Lomnicki S, Dellinger B. Environ. Sci. Technol. 2011; 45:589. [PubMed: 21138295]
7. Vejerano E, Lomnicki SM, Dellinger B. Environ. Sci. Technol. 2012; 46:9406. [PubMed: 22831558]
8. Vejerano E, Lomnicki S, Dellinger B. J. Environ. Monit. 2012; 14:2803. [PubMed: 22990982]
9. Kiruri LW, Khachatryan L, Dellinger B, Lomnicki S. Environ. Sci. Technol. 2014; 48:2212. [PubMed: 24437381]
10. McFerrin CA, Hall RW, Dellinger B. J. Mol. Struct. Theochem. 2008; 848:16.
11. Wichmann HE, Peters A. Philos. Trans. R. Soc. A. 2000; 358:2751.
12. Laden F, Neas LM, Dockery DW, Schwartz JE. Environ. Health Perspect. 2000; 108:941. [PubMed: 11049813]
13. Dellinger B, Pryor WA, Cueto R, Squadrito GL, Hegde V, Deutsch WA. Chem. Res. Toxicol. 2001; 14:1371. [PubMed: 11599928]
14. Pope CA, Burnett RT, Thun MJ, Calle EE, Krewski D, Ito K, Thurston GD. J. Am. Med. Assoc. 2002; 287(9):1132.
15. dela Cruz ALN, Gehling W, Lomnicki S, Cook R, Dellinger B. Environ. Sci. Technol. 2011; 45:6356. [PubMed: 21732664]
16. Balakrishna S, Lomnicki S, McAvey KM, Cole RB, Dellinger B, Cormier SA. Part. Fibre Toxicol. 2009; 6:11. [PubMed: 19374750]
17. Balakrishna S, Saravia J, Thevenot P, Ahlert T, Lominiki S, Dellinger B, Cormier SA. Part. Fibre Toxicol. 2011; 8:11. [PubMed: 21388553]

18. Fahmy B, Ding L, You D, Lomnicki S, Dellinger B, Cormier SA. Environ. Toxicol. Pharmacol. 2010; 29:173. [PubMed: 20369027]
19. Mahne S, Chuang GC, Pankey E, Kiruri L, Kadowitz PJ, Dellinger B, Varner KJ. Am. J. Physiol. Heart Circ. Physiol. 2012; 303:H1135. [PubMed: 22942180]
20. Lord K, Moll D, Lindsey JK, Mahne S, Raman G, Dugas T, Cormier SA, Troxlair D, Lominiki S, Dellinger B, Varner K. J. Recept. Signal Transduct. Res. 2011; 31:157. [PubMed: 21385100]
21. Dulub O, Boatner LA, Diebold U. Surf. Sci. 2002; 519:201.
22. Woll C. Prog. Surf. Sci. 2007; 82:55.
23. Patterson MC, Thibodeaux CA, Kizilkaya O, Kurtz RL, Poliakoff ED, Sprunger PT. Langmuir. 2015; 31:3869. [PubMed: 25774565]
24. Patterson MC, Keilbart ND, Kiruri LW, Thibodeaux CA, Lomnicki S, Kurtz RL, Poliakoff ED, Dellinger B, Sprunger PT. J. Chem. Phys. 2013; 422:277.
25. Kizilkaya O, Jiles RW, Patterson MC, Thibodeaux CA, Poliakoff ED, Sprunger PT, Kurtz RL, Morikawa E. J. Phys. Conf. Ser. 2014; 493:012024.
26. Blaha, P.; Schwarz, K.; Madsen, GKH.; Kvasnicka, D.; Luitz, J. WIEN2k: An Augmented Plane Wave + Local Orbitals Program for Calculating Crystal Properties, Karlheinz Schwarz. Austria: Technische Universitä Wien; 2001. ISBN:3-9501031-1-2.
27. Gopel W, Pollman J, Ivanov I, Reihl B. Phys. Rev. B. 1982; 26:3144.
28. Rangan S, Theisen J-P, Bersch E, Bartynski RA. Appl. Surf. Sci. 2010; 256:4829.
29. Arnaud GF, De Renzi V, del Pennino U, Biagi R, Corradini V, Calzolari A, Ruini A, Catellani A. J. Phys. Chem. C. 2014; 118:3910.
30. Debies TP, Rabalais JW. J. Electron Spectrosc. 1972; 1:355.
31. Zhang Z, Yates JT Jr. Chem. Rev. 2012; 112:5520. [PubMed: 22783915]
32. Rubloff GW, Luth H, Grobman WD. Chem. Phys. Lett. 1976; 39:493.
33. Jones DB, da Silva GB, Neves RFC, Duque HV, Chiari L, de Oliveiria EM, Lopes MCA, da Costa RF, do MT, Varella N, Bettega MHF, Lima MAP, Brunger MJ. J. Phys. Phys. 2014; 141:074314.
34. Ari T, Guven H, Ecevit N. J. Electron Spectrosc. 1995; 73:13.
35. Poss D, Ranke W, Jacobi K. Surf. Sci. 1981; 105:77.

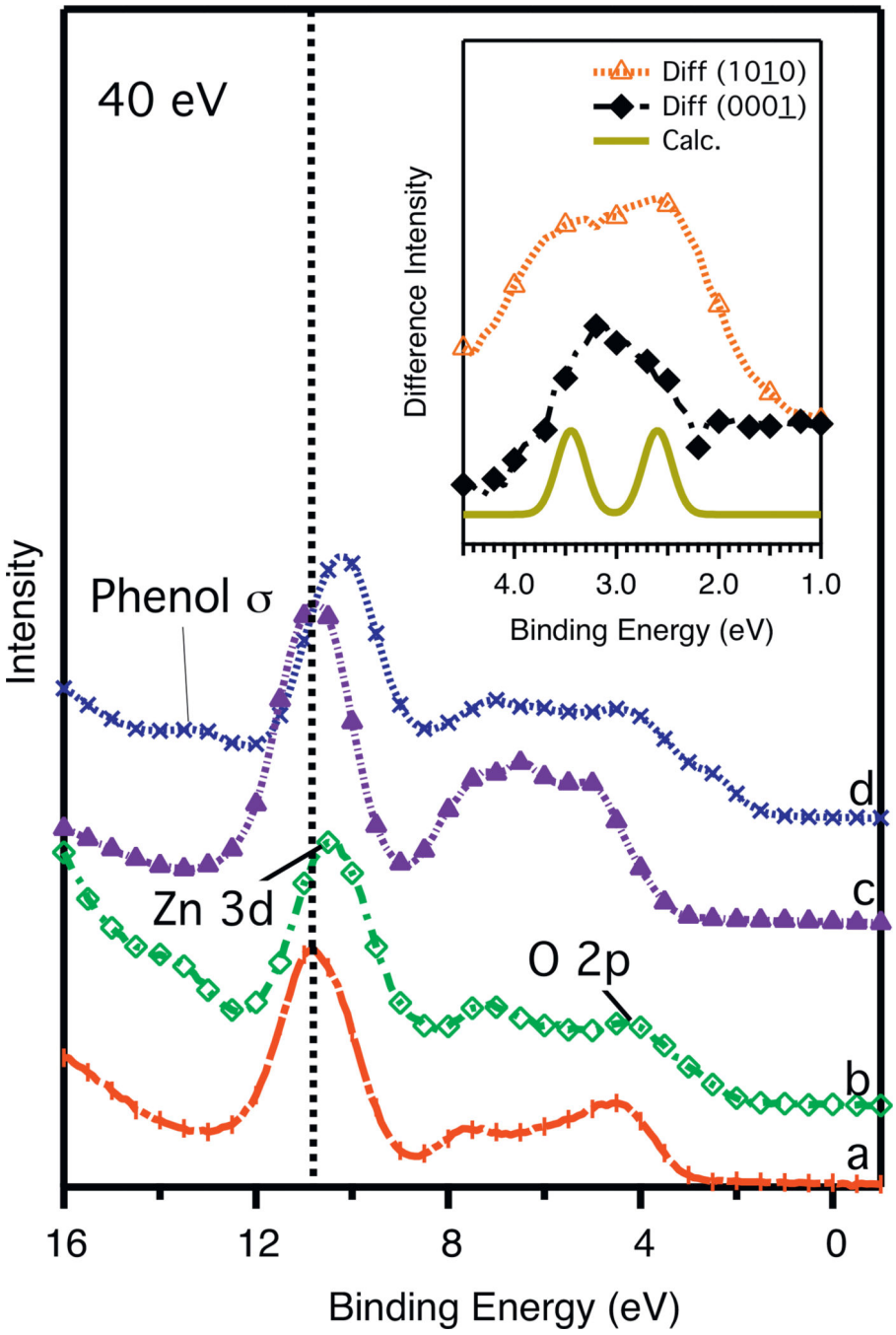

Figure 1.

Room temperature photoelectron spectra of clean and 100 L of phenol dosed ZnO surfaces at 220 °C: (a) clean (0 0 0 $\underline{1}$)-Zn; (b) phenol dosed on (0 0 0 $\underline{1}$)-Zn; (c) clean (1 0 $\underline{1}$ 0); (d) phenol dosed on (1 0 $\underline{1}$ 0) (d). The dashed line at 10.8 eV indicates the center of the Zn *3d* peak on the clean surfaces and consequent band bending of the phenol dosed surfaces. The inset shows the difference spectra in the region between 1 and 4.5 eV (see text for details) as well as calculated spectrum of a fully relaxed phenol molecule (HOMO and HOMO − 1) for comparison.

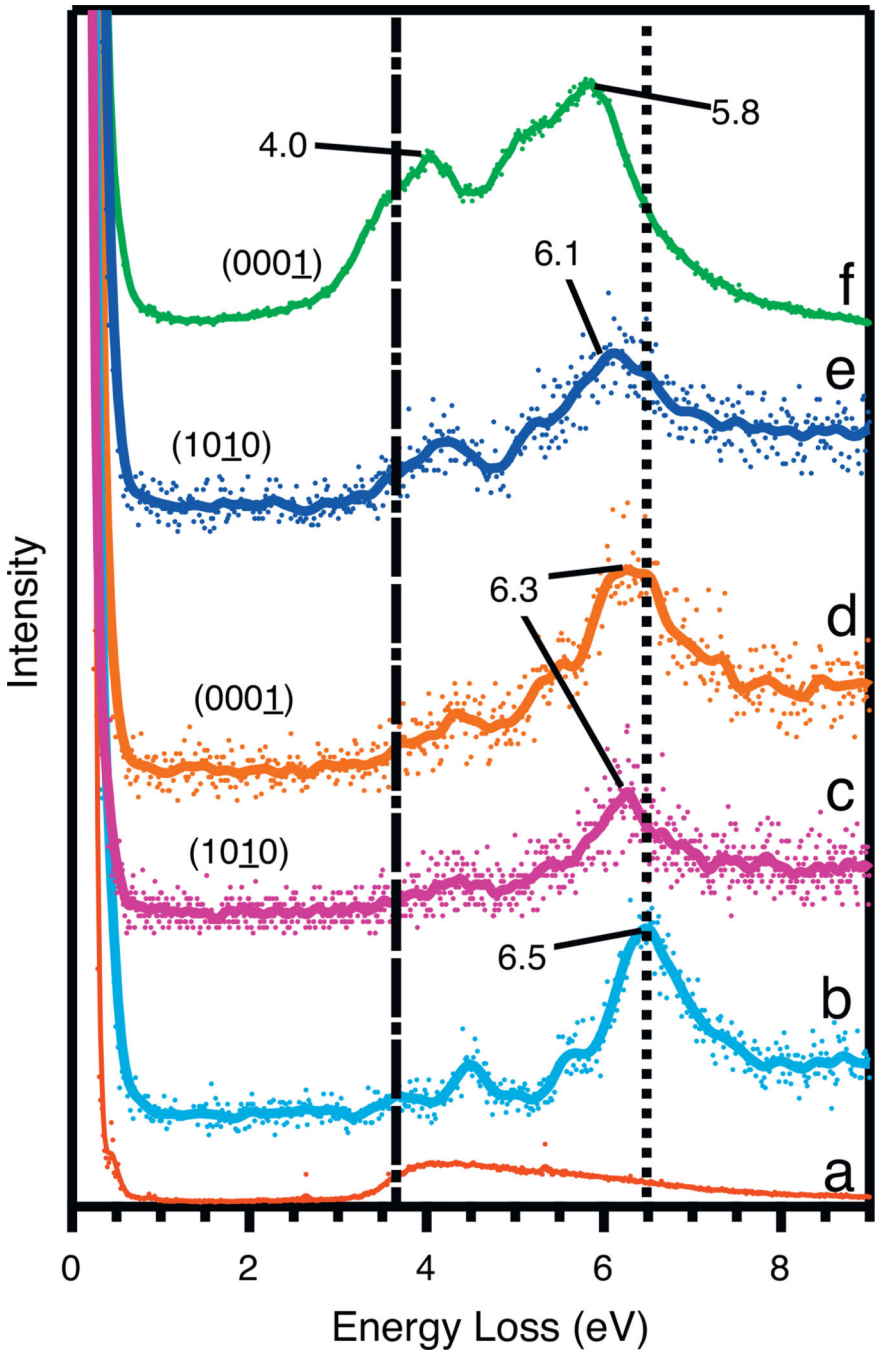

Figure 2.

EELS spectra of 100 L phenol adsorbed to the (1 0 $\underline{1}$ 0) and the (0 0 0 $\underline{1}$)-Zn surfaces at various temperatures. The spectra are as follows: (a) clean (0 0 0 $\underline{1}$)-Zn: (b) adsorption at −177 °C on (1 0 $\underline{1}$ 0); (c) adsorption on (1 0 $\underline{1}$ 0) at room temperature; (d) adsorption on (0 0 0 $\underline{1}$)-Zn at room temperature; (e) adsorption on (1 0 $\underline{1}$ 0) at 220 °C; and (f) adsorption on (0 0 0 $\underline{1}$)-Zn at 220 °C. The dotted vertical line is aligned to the 6.5 eV loss peak of the thick physisorbed phenol layer at −177 °C. The dot-dash vertical line on the left is aligned with

the midpoint of the ZnO band gap at approximately 3.6 eV (a). All spectra are normalized to the elastic peak.

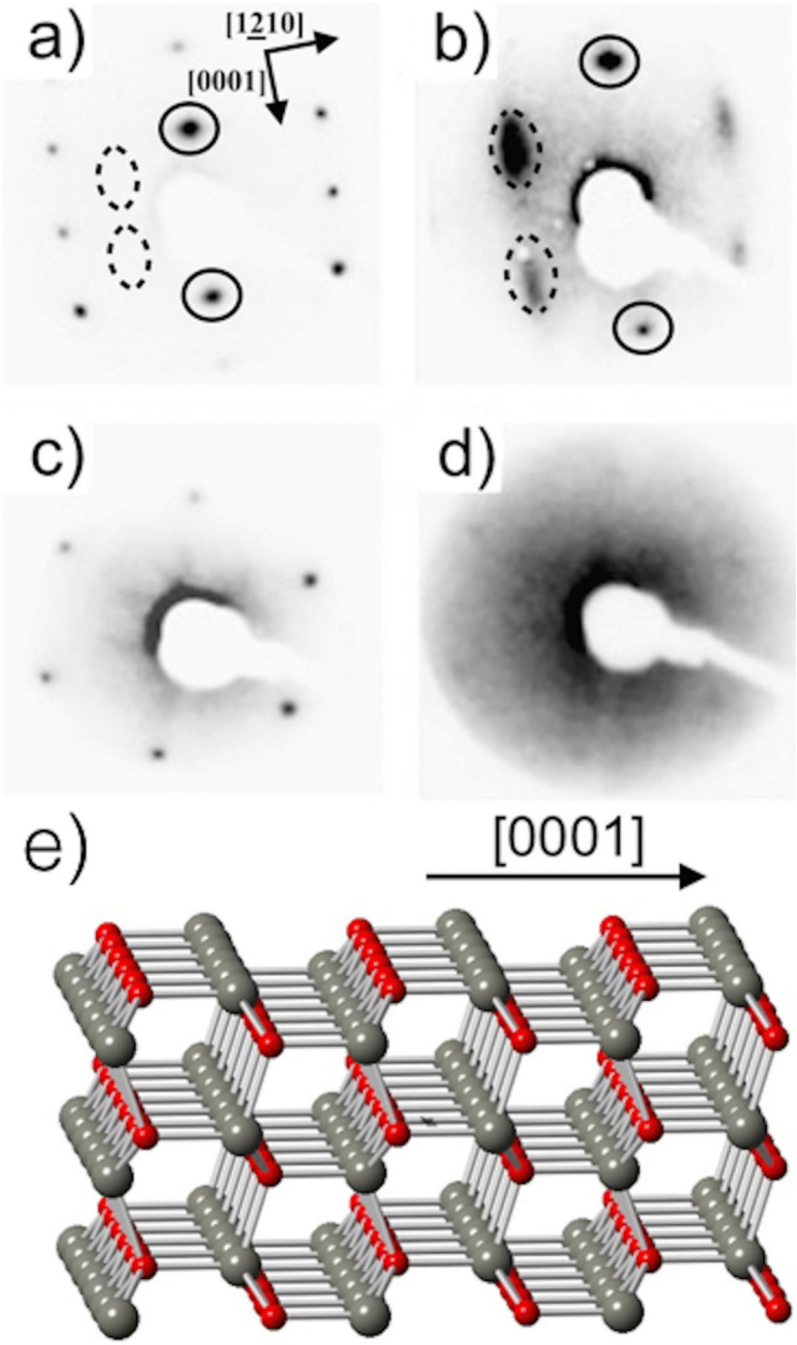

Figure 3.

LEED patterns of: (a) clean (1 0 $\underline{1}$ 0), 69 eV; (b) exposed (1 0 $\underline{1}$ 0) to 25 L phenol at room temperature, 25 eV; (c) clean (0 0 0 $\underline{1}$)-Zn at 69 eV; (d) exposed (0 0 0 $\underline{1}$)-Zn to 25 L phenol at room temperature, 69 eV; (e) structural model of ZnO with arrow indicating the (0 0 0 1) direction The circles in a and b indicate equivalent diffraction spot positions.